

# Journal of Materials Chemistry A

Accepted Manuscript



This is an *Accepted Manuscript*, which has been through the Royal Society of Chemistry peer review process and has been accepted for publication.

*Accepted Manuscripts* are published online shortly after acceptance, before technical editing, formatting and proof reading. Using this free service, authors can make their results available to the community, in citable form, before we publish the edited article. We will replace this *Accepted Manuscript* with the edited and formatted *Advance Article* as soon as it is available.

You can find more information about *Accepted Manuscripts* in the [Information for Authors](#).

Please note that technical editing may introduce minor changes to the text and/or graphics, which may alter content. The journal's standard [Terms & Conditions](#) and the [Ethical guidelines](#) still apply. In no event shall the Royal Society of Chemistry be held responsible for any errors or omissions in this *Accepted Manuscript* or any consequences arising from the use of any information it contains.

Cite this: DOI: 10.1039/c0xx00000x

www.rsc.org/xxxxxx

ARTICLE TYPE

## Enhanced water flux in vertically aligned carbon nanotube array and polyethersulfone composite membranes

Shaoyun Li<sup>a,c</sup>, Gaomin Liao<sup>a,c</sup>, Zhipeng Liu<sup>a,c</sup>, Yuanyuan Pan<sup>a,c</sup>, Qiang Wu<sup>a,b</sup>, Yuyan Weng<sup>c</sup>, Xiaohua Zhang<sup>\*c</sup>, Zhaohui Yang<sup>\*c</sup> and Ophelia K.C. Tsui<sup>d</sup>

Received (in XXX, XXX) Xth XXXXXXXXX 20XX, Accepted Xth XXXXXXXXX 20XX

DOI: 10.1039/b000000x

We describe a novel preparation concept for a unique class of high-flux ultra-filtration membrane comprising a pre-aligned multi-walled carbon nanotube (MWCNT) array and polyethersulfone (PES).

This membrane contains vertically aligned CNTs uniformly distributed inside a PES matrix. The vertically oriented water transportation pathway along the CNTs is verified to facilitate a dramatic enhancement in the water flux through the membrane. The water transportation speed increases about 3 times over the simply mixed CNT/PES membrane with random orientation and more than 10 times over the pure PES membrane under the same pressure load. Low working pressures as well as good retention properties enable this new composite membrane to be an ideal candidate for the future design of high-efficient filtration membrane. This facile technique can potentially be applied to other filtration membrane system to improve the separation efficiency.

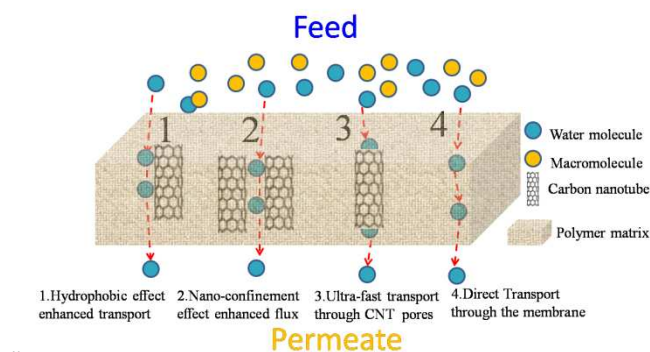
### Introduction

With increasing concern about the growth in world population and limitation in water supply, there is an increasing drive in the water purification industry to find more efficient ways to increase the water supply for human use.<sup>1,2</sup> Filtration techniques by membranes has been deemed more cost and energy effective than other separation methods, such as distillation or absorption.<sup>1,3</sup> The ideal membrane system should possess an excellent stability under a wide range of processing conditions, high selectivity and produce a high mass flux with minimal driving force.<sup>1,2,4</sup> To achieve this goal, both the composition and structure of the membrane are key.

Carbon nanotubes (CNTs) with a one-dimensional tubular structure have been applied as a direct filter<sup>5-7</sup> or effective additive<sup>8,9</sup> to improve such membrane performance as permeability, rejection, disinfection and antifouling behavior. A direct CNT filter is made up of vertically aligned CNTs with open ends extending out of the membrane plane, embedded in an insulate inorganic or organic fillers.<sup>5-7</sup> Nanometer sized CNTs' hollow pores and smooth hydrophobic graphitic walls was hypothesized to serve as the frictionless path for the ultrafast mass transportation (shown as mechanism 3 in scheme 1).<sup>10,11</sup> The water flux rate has been experimentally measured to be 3-4 orders of magnitude faster than the conventional flow estimated from the Hagen-Poiseuille equation.<sup>6,7</sup> The enhancement was attributed to the ballistic motion of water chains (1D wire) inside the CNTs due to the strong hydrogen bonding between the water molecules and minimal interaction with the CNT inner wall.<sup>12,13</sup> However, such vertically aligned CNT filters (referred to as the

VA-CNT filters) requires very high quality CNTs (without any impurity blockage inside the tubes) and complicated end-opening techniques (e.g. plasma etching or argon milling). It is hence not economical for scalable synthesis compared with the conventional mixed matrix membranes.<sup>14</sup>

Meanwhile diffusion along the external surface of the CNTs can also speed up water transportation via hydrophobic effect (shown as mechanism 1 in scheme 1) or nano-confinement effect (mechanism 2).<sup>15</sup> Given the possible mechanisms for water transportation shown in scheme 1, both the miscibility between CNTs and the polymer fillers and the interaction between the water molecules and the CNTs' external walls should affect the membrane permeability.



**Scheme 1.** Illustration of possible pathways for water transportation in a CNT/polymer blend membrane due to (1) hydrophobic effect enhanced transport, (2) nano-confinement enhanced flux, (3) ultrafast transport through the CNT pores, and (4) direct transport through the membrane matrix.<sup>15</sup>

It has been predicted that the permeation coefficient is correlated with the aspect ratio of the CNTs and CNT fraction.<sup>16</sup> In principal, one may attain high permeability by using CNTs with high aspect ratio in large volume fraction. Unfortunately, CNT aggregation always presents a serious problem whether in the mixing of CNTs in a solution or a melt mixture due to the strong van der Waals interaction between the CNTs. Pre-surface modifications of the CNT is thus necessary to improve the compatibility. The relevant effects on the performance of the pre-modified-CNT based composite membrane have been well studied in the literature.<sup>17-20</sup> However, the conventional pretreatment techniques (e.g. acid oxidation treatment) often shorten the length of the CNTs and destroy the external graphitic walls. The rough and hydrophilic CNT's surface may thus trap the water molecules and slow down their motion. The reduced aspect ratio of the shortened CNTs is also unfavorable to the membrane performance.<sup>16</sup>

Relatively few efforts have been spent on proving the performance of CNT/polymer blend membranes by taking advantage of the well-known orientation effects of CNTs towards permeability. The most efficient pathway of CNT blended membrane is predicted when all the CNTs are perpendicular to the membrane plane.<sup>4,14</sup> By using the finite element method, Gusev et al. concluded that the aligned CNTs could accelerate the mass transportation along the CNT direction.<sup>16</sup> In our previous study, the aligned CNT array/hydro-gel system showed an ultra-fast wetting/dewetting behavior,<sup>21</sup> which implies enhanced water transportation and lends support to the concept. Unfortunately, it is a challenge to control the orientation of CNTs in a polymer matrix.<sup>2,14</sup> Dielectrophoresis<sup>22</sup> and special filtration technique<sup>23</sup> can help align the CNTs. However the complicated pre-chemical modification process and relatively low CNT loading impede their developments.

Here we introduce a new strategy to synthesize the high-flux ultra-filtration membrane based on vertically aligned CNT arrays and polyethersulfone (PES) (referred as VA-CNT/PES films) through a simple drop-casting and phase inversion process. The well-aligned arrays of CNTs in the PES matrix are uniformly distributed in the membrane. The PES components exhibit the excellent macromolecule (PEG-20000) rejection property. The water flux in such VA-CNT/PES composite film is measured to be 3 times faster than the CNT/PES membrane in which the CNTs are randomly distributed (referred as R-CNT/PES films), and 10 times faster than the pure PES membrane under the condition. Such enhancement in flux is also obtained when the feeding is a PEG-20000 solution during retention property test. Excellent retention property and stable separation behavior are also found in the VA-CNT/PES membranes. In the following, we shall present data demonstrating these attribute and detail the structure and surface property of these membranes by SEM, TGA, FTIR and contact angle measurements.

Compared to the direct VA-CNT filters, our system does not require the complicated CNTs' end-opening procedure. The retention property relies on the polymer matrix which is convenient to connect with the technologies currently used in the membrane industry. More importantly we can obtain well distributed and aligned CNTs without any pre-modification or post-treatment. Also this technique does not damage the CNT

external walls nor cause the decrease in the aspect ratio of the CNT. The well aligned CNTs form the highly efficient water pathway which facilitates an enhanced water flux and lower pressure consumption. The density and length of the CNTs can be controlled by the CNT growth parameters which may further improve the membrane performance. The new method presented here may shed light on the design of future CNT blend membrane system.

## Results and Discussion

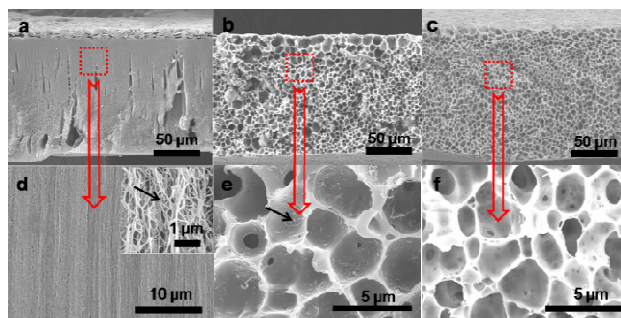


**Figure 1.** The SEM cross section images of the CNT/PES composite membranes under different magnifications, a, d) VA-CNT/PES film; b, e) R-CNT/PES film; c, f) Pure PES film; The black arrow in the inset of fig 1d shows the magnified free space between the CNTs; Another black arrow in fig 1e indicates the isolated carbon nanotubes in the PES matrix.

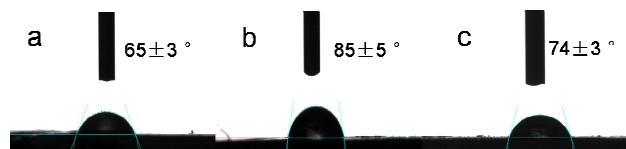
The vertically aligned CNTs obtained here through the CVD method are  $130 \pm 30 \mu\text{m}$  tall with an outer diameter of around 15 nm. (Corresponding TEM images are shown in the Electronic Supplementary Information fig S1) Fig. 1 presents the SEM cross section images of the VA-CNT/PES film (fig 1 a, d), R-CNT/PES film (fig 1 b, e) and pure PES film (fig 1 c, f). For ease of comparison, we chose three kinds of films with a similar thickness of around  $150 \mu\text{m}$ . As fig 1 b shows, the R-CNT/PES film has many macro-void holes with diameters of 5-10  $\mu\text{m}$  due to the phase-inversion process, commonly found in the literature.<sup>27</sup> In the magnified image (fig 1 e), one can see that the CNTs are randomly dispersed inside the PES matrix (as indicated by the black arrow). In the case of the pure PES film (fig 1 c and f), similar macro-void structures form across the whole film. This suggests that addition of the hydrophobic CNTs does not significantly influence the phase inversion behavior of PES. However, a quite different structure is found in the case of the VA-CNT/PES film. As figure 1a shows, two distinctive layers are discernible, indicative of a thin-film composite (TFC) system. We find that the top surface layer with the thickness of  $10 \pm 5 \mu\text{m}$  is composed of PES having the same macro-void structure as the pure PES membrane. The bottom thick layer with a thickness of about  $130 \mu\text{m}$  is a mixture of PES and aligned CNT array. The absence of macro-void structures indicates that the phase inversion process does not occur in bottom layer. One possible explanation is the superhydrophobic VA-CNT array suppresses the phase inversion which causes the formation of the macro-void. From the magnified image shown in fig 1d, the vertically aligned CNTs penetrate the whole membrane, forming a nearly ideal filtration membrane structure as discussed above. As seen in the inset of fig 1d, an inter-connected network of CNTs exists inside PES matrix. There are still spaces between the CNTs and

polymers with a distance of sub-hundred of nanometers (as indicated by the black arrow). We speculate that both the vertically aligned CNT structure and spaces between the CNTs and polymers contribute to the enhancement in flux that will be discussed below.

### Thermal and Spectra analysis

The thermal decomposition analysis of VA-CNT/PES (dash line) and R-CNT/PES (solid line) blend films are shown in Electronic supplementary information fig S3. Similar weight-loss curves in TG graphs and the same peak position in the DTG (Derivative Thermogravimetry) curves demonstrate a similar thermal stability and CNT loading of two films. This verifies the similar chemical nature of the CNTs and the PES fillers in the two membrane systems. From the Raman spectra shown in Electronic supplementary information fig S4 a higher G/D ratio is found in the R-CNT/PES film compared with the VA-CNT/PES film, which indicates a better crystallized graphitic wall in the unmodified commercial CNTs. Fig S5 shows the FT-IR spectra of three types of films. The characteristic vibration peaks at  $1587\text{ cm}^{-1}$  and  $1657\text{ cm}^{-1}$  correspond to the graphitic band of CNT and PES, respectively. No characteristic peaks related to the carboxylic or ester groups are shown in these films. It indicates there is no chemical bonding between the CNTs and the PES fillers.

### Contact angle measurements



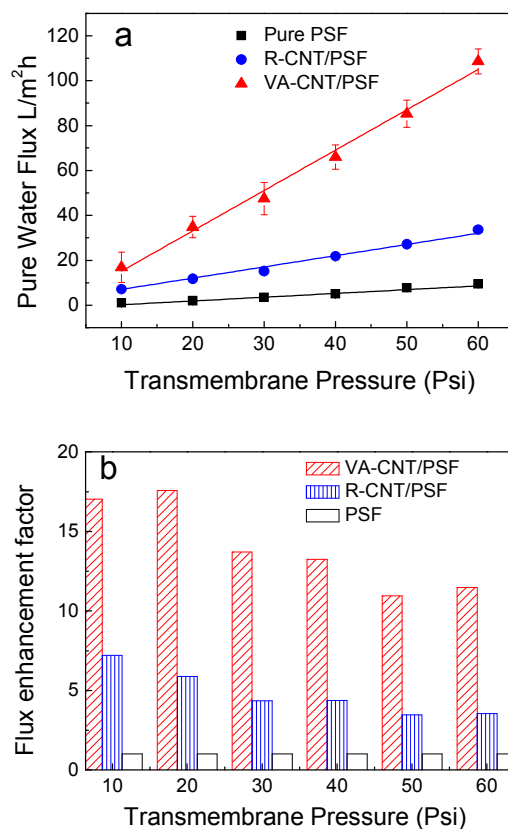
**Figure 2.** Contact angle measurements of three kinds of membranes a) VA-CNT/PES membrane with  $65 \pm 3^\circ$ ; b) R-CNT/PES membrane with  $85 \pm 5^\circ$ ; c) pure PES membrane with  $74 \pm 3^\circ$

Figure 2 shows the contact angle measurement for three types of CNT/PES membranes. Due to the existence of hydrophobic unmodified CNTs in R-CNT/PES film the contact angle of R-CNT/PES film is  $85 \pm 5^\circ$ . The value for the pure PES film is  $74^\circ$ , which is consistent with reported values.<sup>19</sup> The contact angle of VA-CNT/PES film is  $65 \pm 3^\circ$ , indicating the most hydrophilic surface. It is quite abnormal because the as-prepared CNT array is super-hydrophobic, which cannot increase the hydrophilicity of the membrane. It is well known that the surface roughness will affect the wettability of the film.<sup>28</sup> However the surface morphology of the three types of membranes is quite similar from the SEM observations (see Electronic supplementary information part fig S2), which should not significantly influence the surface property. Such a decrease in the contact angle, which can benefit fast water transportation, might be caused by the formation of the well aligned CNT structure in the membrane matrix. In our previous work, composite films consisting of vertically aligned CNTs array in a hydro-gel matrix also exhibited small contact angle with fast wetting and dewetting ability.<sup>21</sup>

### Membrane filtration performance

Figure 3 shows the pure water flux as a function of the transmembrane pressure in the three types of films under the same test

condition. All these samples, the VA-CNT/PES (triangle), R-CNT/PES (circle) and pure PES membranes (square) show a good linear relationship between flux and pressure. Compared with the pure PES film, the R-CNT/PES film shows a water flux enhancement factor of 3-7 which is close to a previous report.<sup>20</sup> It should be emphasized that the CNTs used in the literature have a pre-oxidation treatment that improves the hydrophilicity of the CNTs. Our CNTs are not pre-treated, so the flux increase should be caused by the hydrophobic effect and increase in porosity.<sup>15,19</sup> The extreme hydrophobic surface of the CNTs prevents the water molecule from wetting the polymer pores thus bring a faster transport of water. Also the water molecules may hop from one site to another by interacting with the CNT surfaces due to the rapid sorption and desorption capacity of CNTs,<sup>15</sup> which leads to a fast transport of water molecules along the CNTs surface. More importantly, the VA-CNT/PES film exhibits an even better water transportation ability as compared with the R-CNT/PES film. The flux enhancement factor of VA-CNT/PES membranes is calculated to be 2.4 to 3.3 (depending on the working pressure, see Fig. 3b) over the R-CNT/PES film and 10 to 17 (depending on the working pressure, see Fig. 3b) over the pure PES film under the same conditions. Theoretical simulations have predicted a flux enhancement factor of 3 for gas transportation caused by the alignment of CNTs.<sup>16</sup> In our case the enhancement factor of VA-CNT/PES film versus R-CNT/PES film is close to the simulation result.



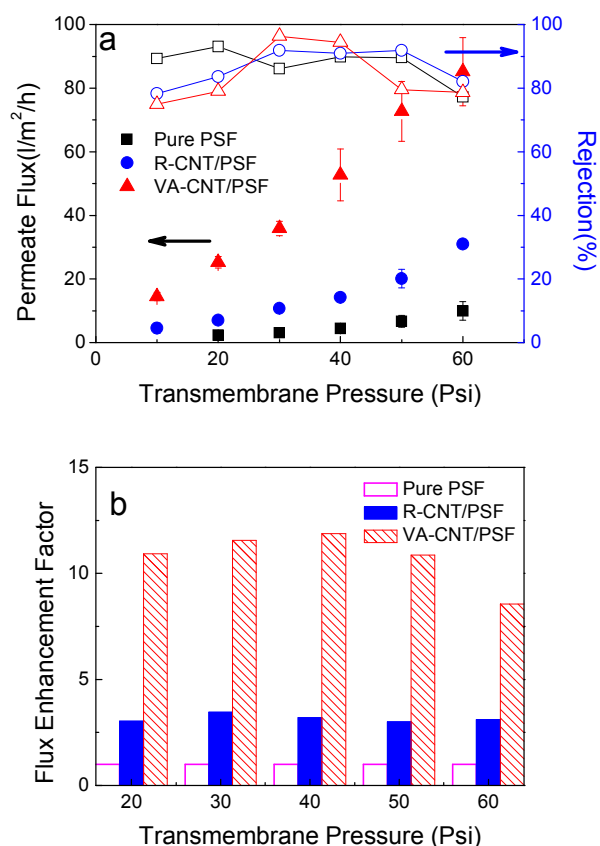
**Figure 3.** a) Pure water flux of the VA-CNT/PES (triangle), R-CNT/PES (circle) blend membrane and pure PES membrane (square) as a function of the working pressure. b) The flux enhancement factor in the different

type of CNT/PES membranes at different working pressures (The flux in the pure PES membrane is set as the standard.)

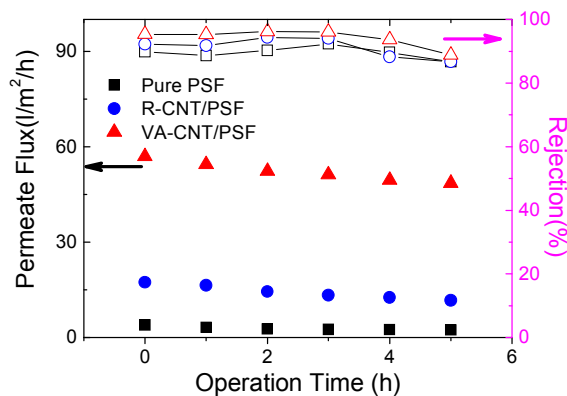
Generally the water flux has a direct relationship with the membrane porosity.<sup>29</sup> The porosity of the R-CNT/PES film is 5 (59% ± 5%) while the value for the pure PES is (40% ± 3%). Interestingly, porosity of the VA-CNT/PES film is (52% ± 5%) although it does not show an obvious macro void structure. This observation can be explained as the numerous nano-meter sized free spaces between the CNT array and the PES matrix (as shown 10 in fig 1d).<sup>21</sup> Although the porosity of the VA-CNT/PES film is smaller as compared to the R-CNT/PES film a flux enhancement (the flux enhancement factor is around 3) is observed in the VA-CNT/PES system. The acceleration mechanism is thus ascribed to the vertically aligned CNT structure as well as interconnected 15 hydrophobic free spaces between the CNTs and polymer fillers rather than the porosity increase. It indicates water molecules transfer along these efficient pathways through the membrane with a relatively high speed as shown in scheme 1.

The retention test is carried out on the same ultra-filtration cell 20 with PEG-20000 as the feeding solution. As figure 4a shows, the three kinds of films show a rejection property of 75-95% at different applied pressures. An optimized working pressure in the VA-CNT/PES film is 40 psi with a rejection rate of 95%. Under this condition, the permeate flux in the VA-CNT/PES film is 25 measured to be 3.7 times higher than the R-CNT/PES film and 12 times higher than the pure PES film. The mechanism of the enhancement is similar to that discussed above. Based on Fig. 4a the rejection rate of the two CNT-containing films increases with increasing pressure and reaches a maximum at 30 psi whereas the 30 pure PSF film shows the best retention performance at 20 psi. This phenomenon is similar to the observation by Choi *et al.* and probably caused by the PSF surface fouling of the PEG molecules.<sup>18</sup> It indicates the formation of a relatively compact PEG layer at higher operating pressure which probably suppress 35 the transport of the solute. The rejection rate then decreases with further increase in the applied pressure due to the increasing concentration polarization effect.<sup>18</sup> Meanwhile the permeate flux increases with the pressure monotonically but does not follow a linear relation. This may be caused by the alternation of the pore 40 structure under high pressure and change in the surface property of the CNTs (*e.g.* the PEG molecules adsorbing onto the CNTs).

To test the durability of the composite membrane, we record the time sequenced permeate flux at a constant pressure of 40 psi. As Fig. 5 shows, the flux (solid labels) in the three types of the 45 membranes all decreases with time and eventually reaches an equilibrium value. The decrease in the flux after a 5-hour running is calculated to be 27% for the VA-CNT/PES film, 58% for the R-CNT/PES film and 81% for the pure PES film. As a smaller decrease of flux usually indicates a better anti-fouling ability,<sup>30</sup> the VA-CNT/PES film shows an improved anti-fouling property 50 compared with the other two membranes. Meanwhile the rejection rate (hollow labels) maintains at a high constant level (around 90% for R-CNT/PES film, 89% for pure PES film and 95% for VA-CNT/PES film) and only starts to decrease after 4-5 hours operation. The decrease of the flux can be ascribed to the adsorption of PEG molecules on the membrane surface which forms a cake-like layer during the permeation process.<sup>30</sup>



60 **Figure 4.** a) Water flux (left) and retention (right) behavior of the three kinds of membrane discussed in the text towards a 50 mg/L PEG-20000 solution, triangle: VA-CNT/PES, circle: R-CNT/PES, square: pure PES membrane. b) Flux enhanced factor for the three kinds of membranes at different pressures. Sparse: VA-CNT/PES, solid: R-CNT/PES, hollow: 65 pure PES membrane. The flux in the pure PES membrane is set as the standard.



70 **Figure 5.** Time sequenced permeate flux (solid symbols) and rejection (hollow symbols) of three type of PES membranes at the working pressure of 40 psi, VA-CNT/PES (triangle), R-CNT/PES (circle) and pure PES membrane (square)

## Experimental Section

### Materials

Polyethersulfone resin (PES, Mw = 75000 g/mol) was supplied

by Acros Organics. Polyethylene glycol (PEG, Mw = 20000 g/mol) and polyvinylpyrrolidone (PVP, Mw = 58000 g/mol) were purchased from Aladdin Chemistry (Shanghai, China). MWNT powders were obtained from Shenzhen Nanotech Port, Shenzhen China (15 nm O.D., 5-10  $\mu$ m in length). Other chemicals were obtained from Sinopharm Chemical Reagent (Shanghai, China) without further purification.

### Characterization

The morphology of the CNT/PES composite membranes was examined by scanning electron microscopy (Hitachi S-4700, Japan). Cross-sectional images were obtained after fracturing the membranes in liquid nitrogen. A Tecnai G220 (FEI) transmission electron microscope (TEM) operated at a 180 KV accelerating voltage was used.

Thermo gravimetric analyzer (TGA) (SII EXSTAR TG/DTA 6300) was utilized to investigate the thermal weight loss of samples in a nitrogen environment by heating up to 800 °C with a heating rate of 20°C/min.

The contact angle measurement was carried out on a contact angle goniometer (OCA20, Dataphysics, Germany) equipped with a video camera at room temperature to check the hydrophilicity of the membrane surface. Three samples were measured to get an average result.

The FTIR spectra are obtained through the Nicolet 6700 FT-IR spectrophotometer. The Raman spectra are measured on a Raman Spectrophotometer (HR800, HORIBA Jobin Yvon Company) excited by a laser with wavelength of 632.8 nm.

### Preparation of vertically aligned CNT array

The vertically aligned CNT array was grown through a conventional chemical vapor deposition (CVD) method with Fe/Al thin film pre-deposited as the catalyst via E-beam evaporation.<sup>24</sup> The height and density of the array can be controlled by the growth parameters.

### Preparation of the R-CNT/PES, pure PES and VA-CNT/PES membrane

Preparation of the R-CNT/PES membrane is based on what is reported in the literature with some modification.<sup>18,25</sup> The precursor solution containing 14 wt % PES and 2 wt% PVP (used as the porogen) in N-methyl pyrrolidone (NMP) is continuously stirred for 2 hours to form a homogeneous solution. Then it is mixed with 1 wt% MWCNT powder followed by strong ultrasonication over 3 hours. After storing for 24 hours to remove air bubbles, 0.5 ml solution is drop-coated onto the surface of a 2cm  $\times$  5cm clean glass slide and then transferred to a coagulating water bath to get the free standing film. After thoroughly rinsing with DI water, the membrane is dried for 12 hours at room temperature and stored in DI-water for further test.

To prepare the pure PES membrane the same amount of precursor solution (without CNTs) is drop-coated and treated with the same procedure.

To prepare the VA-CNT/PES membrane, 0.05 ml precursor solution (without CNTs) is drop-coated onto the surface of a CNT array film (about 1cm $\times$ 1cm in area) and treated with the same procedure as mentioned above. The VA-CNT/PES membrane is very easily peeled off from the silicon substrate after the immersion in the coagulation bath.

### Porosity measurement

Membrane porosity is measured through the “dry-wet weight loss” method.<sup>26</sup> Details can be found in the Electronic Supplementary Information part.

### Membrane performance test

An ultra-filtration test system is designed as shown in Electronic Supplementary Information scheme S2 to evaluate the filtration performance of the CNT composite membranes. All filtration experiments are conducted at a constant transmembrane pressure between 10-60 psi with a system temperature of 20 °C. Each membrane is placed on a porous stainless steel disk with the active membrane area of 1.54 cm<sup>2</sup> for pure PES membrane and R-CNT/PES membrane and 0.38 cm<sup>2</sup> for VA-CNT/PES membrane. Pure DI water and an aqueous solution of PEG-20000 (50 mg/L) are used as the feedings. The data are recorded after 30 min pre-treatment at the working pressure. Each film is tested at least for 5 samples to get an average result. Details of this experiment can be found in the Electronic Supplementary Information.

### Conclusions

In conclusion, we have designed and fabricated a new type of ultra-filtration membrane based on the vertically aligned MWCNT array/PES composites. The uniqueness of this membrane is the orderly alignment of CNTs inside the polymer matrix which provides the ultra-efficient pathway for water transportation. The promising enhancement in the water flux verifies the theoretical prediction of the acceleration effect caused by the aligned CNTs. The good retention behavior and stable separation property benefit the separation efficiency of this aligned CNT array/PES blend membrane. In the future work, the array height and density, the CNT diameter as well as the surface property, will be precisely controlled to further improve the membrane performance. This technique might show potential to be used in other ultra-filtration, nano-filtration and reverse osmosis systems.

### Acknowledgements

This work was financially supported by the National Basic Research Program of China (973Program) (No. 2012CB821505), National Natural Science Foundation of China (No.91027040,21204059,21204058,21274103,21104054), Natural Science Foundation of Jiangsu Province (No. BK2011300). The authors also thank for the Specially-Appointed Professor Plan in Jiangsu Province (No.SR10800312) and Project for Jiangsu Scientific and Technological Innovation team(2013). Prof. F. Zhu-ge, Mr. B. Fu from Ningbo Institute of Materials Technology & Engineering (Chinese Academy of Sciences) and Mr. L. Li from ULVAC (Suzhou) Co.LTD for the help of E-beam evaporation experiment were also greatly acknowledged. We also thank Prof. J. Meng from Tianjin Polytechnic University for the helpful discussion.

### Notes and references

a. Department of Polymer Science and Engineering, College of Chemistry, Chemical Engineering and Materials Science, Soochow University

b. Physics Department, Soochow University

c. Center for Soft Condensed Matter Physics and Interdisciplinary Research, Soochow University, Suzhou, 215006, P.R. China

d. Physics Department, Boston University, Boston, MA, 02134

E-mail: yangzhaohui@suda.edu.cn; zhangxiaohua@suda.edu.cn

Electronic Supplementary Information (ESI) available: Evaluation of membrane performance, porosity measurement, schematic representation of the enhanced water transportation in different CNT blended membrane(scheme s1), schematic diagram of the device for the permeation tests(scheme s2), TEM images of as-prepared CNTs(figure s1), SEM images of the surface morphology of three type of CNT/PES membranes(figure s2), TGA and SDT analysis of R-CNT/PES film and VA-CNT/PES film(figure s3), Raman(figure s4) and FTIR (figure s5)spectra of the blend membrane and standard curves of PEG 20000 with the iodine staining(figure s6) shown here. See DOI: 10.1039/b000000x/

## Notes

This work is dedicated to Professor Weixiao Cao, Peking University, China, for his 80<sup>th</sup> birthday in November 2014

1. M. Elimelech, W. A. Phillip, *Science* 2011, **333**, 712.
2. Shannon, M. A.; Bohn, P. W.; Elimelech, M.; Georgiadis, J. G.; Mariñas, B. J.; Mayes, A. M. *Nature*, 2008, **452**, 301.
3. Li, D.; Wang, H., *J. Mater. Chem.* 2010, **20**, 4551.
4. M.T.M. Pendergast, E.M.V. Hoek, *Energ. Environ. Sci.* 2011, **4**, 1946.
5. B. J. Hinds, N. Chopra, T. Rantell, R. Andrews, V. Gavalas, L. G. Bachas, *Science* 2004, **303**, 62.
6. M. Majumder, N. Chopra, R. Andrews, B. J. Hinds, *Nature*, 2005, **438**, 44.
7. J. K. Holt, H. G. Park, Y. Wang, M. Stadermann, A. B. Artyukhin, C. P. Grigoropoulos, A. Noy, O. Bakajin, *Science* 2006, **312**, 1034.
8. C. H. Ahn, Y. Baek, C. Lee, S. O. Kim, S. Kim, S. Lee, S.H. Kim, S. S. Bae, J. Park, J. Yoon, *J. Ind. Eng. Chem.* 2012, **18**, 1551.
9. S. Kar, R. C. Bindal, P. K. Tewari, *Nano Today* 2012, **7**, 385.
10. G. Hummer, J. C. Rasaiah, J. P. Noworyta, *Nature* 2001, **414**, 188.
11. A. Kalra, S. Garde, G. Hummer, *Proc. Nat. Acad. Sci. USA* 2003, **100**, 10175.
12. A. Noy, H. G. Park, F. Fornasiero, J. K. Holt, C. P. Grigoropoulos, O. Bakajin, *Nano Today* 2007, **2**, 22.
13. S. Joseph, N. R. Aluru, *Nano Lett.* 2008, **8**, 452.
14. D. S. Sholl, J. K. Johnson, *Science* 2006, **312**, 1003.
15. K. Gethard, O. Sae-Khow, S. Mitra, *ACS applied materials & interfaces* 2010, **3**, 110.
16. A. A. Gusev, O. Guseva, *Adv. Mater.* 2007, **19**, 2672.
17. C.F. De Lannoy, E. Soyer, M. R. Wiesner, *J. Membr. Sci.* 2013, **447**, 395.
18. J.H. Choi, J. Jegal, W.N. Kim, *J. Membr. Sci.* 2006, **284**, 406.
19. S. Qiu, L. Wu, X. Pan, L. Zhang, H. Chen, C. Gao, *J. Membr. Sci.* 2009, **342**, 165.
20. E. Celik, H. Park, H. Choi, H. Choi, *Water Res.* 2011, **45**, 274.
21. Z. Yang, Z. Cao, H. Sun, Y. Li, *Adv. Mater.* 2008, **20**, 2201.
22. S. Shekhar, P. Stokes, S. I. Khondaker, *ACS Nano* 2011, **5**, 1739.
23. S. Kim, J. R. Jinschek, H. Chen, D. S. Sholl, E. Marand, *Nano Lett.* 2007, **7**, 2806.
24. Z. Liu, G. Liao, S. Li, Y. Pan, X. Wang, Y. Weng, X. Zhang, Z. Yang, *J. Mater. Chem. A* 2013, **1**, 13321.
25. S. Maphutha, K. Moothi, M. Meyyappan, S. E. Iyuke, *Sci. Rep.* 2013, **3**, 1509.
26. Y. Ma, F. Shi, Z. Wang, M. Wu, J. Ma, C. Gao, *Desalination* 2012, **286**, 131.
27. Y. Medina-Gonzalez, J. C. Remigy, *Mater. Lett.* 2011, **65**, 229.
28. D. Quere, *Annu. Rev. Mater. Res.* 2008, **38**, 71.
29. M.J. Han, S.T. Nam, *J. Membr. Sci.* 2002, **202**, 55.
30. J. Yin, G. Zhu, B. Deng, *J. Membr. Sci.* 2013, **437**, 237.

70